Journal of Applied Polymer Science

# Utilization of Waste Polystyrene and Starch for Superabsorbent Composite Preparation

**Hanafi Ismail, Maryam Irani, Zulkifli Ahmad**

Division of Polymer Engineering, School of Materials and Mineral Resources Engineering, USM Engineering Campus, Universiti Sains Malaysia, 14300 Nibong Tebal, Penang, Malaysia

Correspondence to: H. Ismail (E-mail: hanafi@eng.usm.my)

**ABSTRACT:** A superabsorbent composed of waste polystyrene, starch, and acrylic acid was prepared through emulsion polymerization. The effects of major factors such as starch, acrylic acid, initiator, crosslinker, and bentonite contents and the neutralization degree of acrylic acid on water absorbency were investigated to obtain optimum conditions with high swelling capacity. The superabsorbent hydrogel was characterized by scanning electron microscope (SEM), Fourier transform infrared (FTIR) spectroscopy, and thermogravimetric analysis (TGA). The FTIR results confirmed that the grafting polymerization took place among the polystyrene, acrylic acid, starch, and bentonite. The introduction of bentonite particles into the polystyrene-*g*-poly (acrylic acid)-*co*-starch system could increase the water absorbency. The superabsorbent composite containing 3 wt % bentonite had the highest water absorbency (500 g/g in distilled water and 49 g/g in 0.9 wt % NaCl solution). © 2012 Wiley Periodicals, Inc. J. Appl. Polym. Sci. 000: 000–000, 2012

**KEYWORDS:** waste polystyrene; superabsorbent hydrogel; starch

Received 9 March 2012; accepted 24 April 2012; published online
**DOI: 10.1002/app.37952**

## INTRODUCTION

Polystyrene is a synthetic hydrophobic polymer that is not biodegradable. Thus, it can cause environmental pollution.[1] There are different alternatives for reducing the problem of its disposal and for converting it into valuable products, including polymer modification and functionalization.[2,3] The introduction of polar groups into synthetic polymers causes the induction of hydrophilicity.[4,5] Functionalized polystyrene has different applications, for instance, as a polyelectrolyte for water treatment processes.[6]

Studies have been reported on the preparation of superabsorbent hydrogels using natural polymers such as starch, wheat straw, and chitosan.[7–9] In recent years, more attention has been given to the modification of synthetic polymers with natural polymers such as wool, gelatin, and starch.[10] Starch is a natural polymer and is an inexpensive, abundant, and renewable resource. The chemical modification of starch via hydrolysis, oxidation, esterification, and etherification has been studied previously.[11] In addition, the grafting of acrylic acid,[12,13] acrylamide,[11,14] acrylonitrile,[15] and methacrylonitrile[16] onto starch has been studied. Starch copolymers have been important due to their potential applications in industry. For example, starch copolymers have been used as hydrogels. Recently, superabsorbent hydrogels have received more attention due to their various applications in agriculture,[17–20] drug delivery systems, biomedical uses,[21,22] coal dewatering,[23] and sanitary goods.[24] In recent years, different types of clays have been used for the preparation of superabsorbent composites to enhance swelling properties and hydrogel strength, and to decrease the production cost of prepared superabsorbents such as kaolin,[25] montmorillonite,[9] attapulgite,[17,26] and mica.[27] The clay used in this work is bentonite, due to its low cost and natural abundance. Bentonite is a sheet-like clay and is mainly composed of the mineral montmorillonite, a 2 : 1-type of alumina silicate.

Li and coworkers prepared a superabsorbent composite using waste polystyrene, acrylic acid, and montmorillonite through emulsion polymerization.[28] Singh et al. synthesized polystyrene graft copolymers using acrylic acid and starch through graft copolymerization, and they investigated its application in metal ion sorption for use in water alleviation technology.[10] The copolymerization of starch and polystyrene has been carried out in a twin-screw extruder to form partially biodegradable plastic.[29] However, to the best of the authors' knowledge, no work has been performed with waste polystyrene and starch for the preparation of superabsorbent hydrogel. In this work, the purpose was to prepare superabsorbent hydrogel using waste polystyrene, starch, and bentonite to reduce the cost of the final

product, and to help decrease environmental problems with waste polystyrene.

## EXPERIMENTAL

### Materials

Potassium persulfate (KPS), benzoyl peroxide (BP), and sodium hydroxide were obtained from Merck. Acrylic acid (AA, from Fluka) was used without purification. Toluene, *n*-hexane, and ethylene acetate were obtained from Merck. Waste polystyrene foam (from food containers) was washed with distilled water before use. *N*,*N*′-methylene-bis-acrylamide (MBA) and Span 60 were purchased from Aldrich. Cassava starch (food grade) was obtained from Thye Huat Chan Sdn BhD, Thailand. Bentonite (BT) was supplied by Ipoh Ceramics Sdn. Bhd.

### Instrumental Analysis

FTIR spectra of the prepared samples were taken with KBr pellets using a Perkin Elmer Spectrum One apparatus. The FTIR spectra of the samples were obtained for a range from 4000 to 550 $cm^{-1}$.

Thermogravimetric analysis (TGA) of the composites was carried out with a Perkin Elmer Pyris 6 TGA analyzer from 50 to 700°C with a nitrogen flow of 10 mL $min^{-1}$.

Micrographs of the prepared superabsorbents were collected using a field emission scanning electron microscope (FESEM, ZEISS Supra-35VP). Before SEM observation, the samples were coated with a thin layer of platinum.

### Preparation of Na-Bentonite

The Na-bentonite ($Na^+$-BT) was prepared by stirring 5 g of the sample in 500 mL of 1.0*M* NaCl solution for 24 h. The $Na^+$-BT was separated from excess solution by centrifugation and washed with distilled water several times to remove $Cl^-$. Then, the product was dried at a temperature of 105°C over night.[30]

### Preparation of Polystyrene-Graft-Poly (Acrylic Acid)-*co*-Starch/Bentonite (PS-*g*-PAA-*co*-ST/BT) Superabsorbent Hydrogel

The preparation of PS-*g*-PAA-*co*-ST/BT included four steps. In the first step, a proper amount of waste polystyrene (PS) was dissolved in a mixture of solvents including *n*-hexane, toluene, and ethyl acetate. Appropriate amounts of Span 60 (as an emulsifier) and an oil-soluble initiator, benzoyl peroxide (BP), were added to the solution in a four-necked reaction flask equipped with a thermometer, a mechanical stirrer, and a nitrogen line. In the second step, a definite amount of acrylic acid (AA) was partially neutralized with sodium hydroxide solution (3*M*) with cooling (ice bath), and a proper amount of $Na^+$-BT was added to the acrylic acid solution under stirring for a few minutes. Then the acrylic acid solution was added to the reaction flask and heated to 45°C for a few minutes. In the third step, a proper amount of starch (ST) combined with distilled water was heated to 90°C under a nitrogen atmosphere to prepare a starch slurry. Then, the starch slurry was added to the flask, and the solution was heated to 60°C. In the fourth step, appropriate amounts of crosslinker (MBA) and initiator (potassium persulfate) were added to the solution; after a few minutes, the temperature was increased to 70°C for 2 h. Then the samples were precipitated into the ethanol, filtered, cut into small pieces, and dried at 80°C for 12 h, followed by milling and screening. Acrylic acid homopolymers and unreacted monomers were extracted from the product by soxhlet extraction using an ethanol–water mixture (80: 20) for 8 h.[31] The extraction was carried out three times for the samples to obtain the constant weight of grafted samples.

### Preparation of the PS-*g*-PAA-*co*-ST Superabsorbent Hydrogel

The preparation method of the PS-*g*-PAA-*co*-ST superabsorbent hydrogel used herein is similar to that of the PS-*g*-PAA-*co*-ST/BT superabsorbent composite except that bentonite was not included.

### Water Absorbency Measurement

A certain amount of sample (0.1 ± 0.01 g) with particle sizes between 60 and 100 mesh (150–250 $\mu$m) was immersed in 50 mL of saline solution (0.9 wt %) or 200 mL of distilled water, and the samples were allowed to soak at room temperature for 3 h. Then swollen samples were separated from excess water by filtering via a 100-mesh screen, and the samples were weighed. The swelling absorbency ($Q_{H2O}$) of the sample was calculated using the following formula:

$$Q_{H2O} = (m_2 - m_1)/m_1 \quad (1)$$

where $m_2$ and $m_1$ are the weights of swelling gel and dried gel, respectively.

## RESULTS AND DISCUSSION

### FTIR Spectrum Analysis

The FTIR spectra of BT, starch, PS-*g*-PAA-*co*-ST and PS-*g*-PAA-*co*-ST/BT are shown in Figure 1. In the spectrum of starch, the broad band at 3389 $cm^{-1}$ arises due to the stretching band of the O—H groups. The band at 1642 $cm^{-1}$ is related to the first overtone of the O—H bending vibration. The bands at 2927 and 1156 $cm^{-1}$ result from C—H stretching and C—O stretching, respectively. The two bands at 1079 and 1015 $cm^{-1}$ are related to $CH_2$—O—$CH_2$ stretching vibrations.[32] The spectrum of Na-BT shows a band at 3626 $cm^{-1}$, which is a result of the O—H stretching vibrations of Si—OH groups.[30] The band at 3450 $cm^{-1}$ is due to hydroxyls bound via hydrogen bonds. The band at 1633 $cm^{-1}$ corresponds to the H—O—H bending vibration in water. The band arising from Al—Al—OH is shown at 915 $cm^{-1}$.[33] The bands at 463 and 520 $cm^{-1}$ correspond to the Si—O—Si and Al—O—Si bending vibrations, respectively. According to the FTIR spectra of PS-*g*-PAA-*co*-ST, the band at 2923 $cm^{-1}$ corresponds to the asymmetric and symmetric stretching vibrations of —$CH_2$ from PS. The peak at 1585 $cm^{-1}$ is due to the C=C of the vinyl group from PS while the band at 1452 $cm^{-1}$ results from the deformational vibrations of —$CH_2$ and (B1) of the benzene ring of the styrene molecule.[34] The band at 1734 $cm^{-1}$ corresponds to the asymmetrical C=O stretching band of AA. The band at 1412 $cm^{-1}$ is due to the $COO^-$ of AA. The broad absorption band at 3468 $cm^{-1}$ corresponds to the OH stretching of starch. Additionally, the absorption band at 1156 $cm^{-1}$ ascribed to the C—O band of starch was overlapped by the C—O band of acrylic acid shifted to 1169 $cm^{-1}$, and it appears to be broader than that of starch.

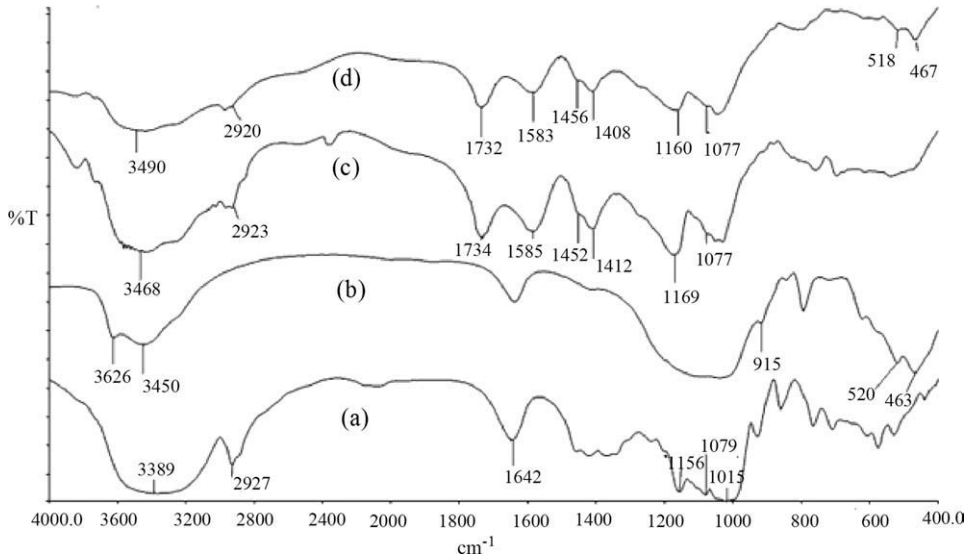


**Figure 1.** FTIR spectra of (a) starch, (b) sodium bentonite, (c) PS-*g*-PAA-*co*-ST, and (d) PS-*g*-PAA-*co*-ST/BT.

The absorption bands at 3626, 3450, and 912 $cm^{-1}$ corresponding to the —OH of BT were not observed in the spectrum of PS-*g*-PAA-*co*-ST/BT in comparison to that of BT. Furthermore, the absorption bands at 460 and 520 $cm^{-1}$ ascribed to the Si—O—Si and Al—O—Si of BT shifted to 467 and 518 $cm^{-1}$, respectively, and the intensity decreased. These results show the participation of the —OH groups of BT in the formation of the composite. After BT was introduced into the polymeric network, the absorption bands of the $—COO^-$ groups shifted from 1412 to 1408 $cm^{-1}$, which shows that the chemical environment of the $—COO^-$ groups was altered. In addition, the absorption band at 1169 $cm^{-1}$ ascribed to the C—O of starch and acrylic acid in the spectrum of PS-*g*-PAA-*co*-ST shifted to 1160 $cm^{-1}$ and decreased in intensity, indicating that there may be a hydrogen bonding between the surface silanol groups of Na—B and the —C—O group of PS-*g*-PAA-*co*-ST. It can be concluded from Figure 1 that grafting polymerization took place among the polystyrene, acrylic acid, starch and bentonite.

### Mechanism of Hydrogel Formation

Crosslinking graft copolymerization of starch and acrylic acid onto polystyrene was carried out in the presence of a bi-phase initiator system including an oil-soluble initiator (benzoyl peroxide) and a water-soluble initiator (potassium persulfate). In addition, MBA was used as a crosslinker. A proposed mechanism for the formation of PS-*g*-PAA-*co*-ST is shown in Figure 2. Benzoyl peroxide as an oil-soluble initiator can be decomposed under heating to produce benzoate radicals. One possible type of hydrogen abstraction on the polystyrene backbone can occur on the tertiary carbon atoms of polystyrene chains to produce tertiary benzylic radicals,[35] as shown in Figure 2. These active centers on the backbone chains can initiate the grafting of AA, and starch on PS. After KPS and MBA were added to the reaction flask and heated slowly to 60°C, the water-soluble initiator decomposed to produce sulfate anion radicals. It should be mentioned that a second initiator (KPS in this system) is used to complete the reaction. In addition, the amount of the first initiator is not sufficient to complete the polymerization of the material present in the solution, so the second initiator is used to decrease the residual-free monomer content

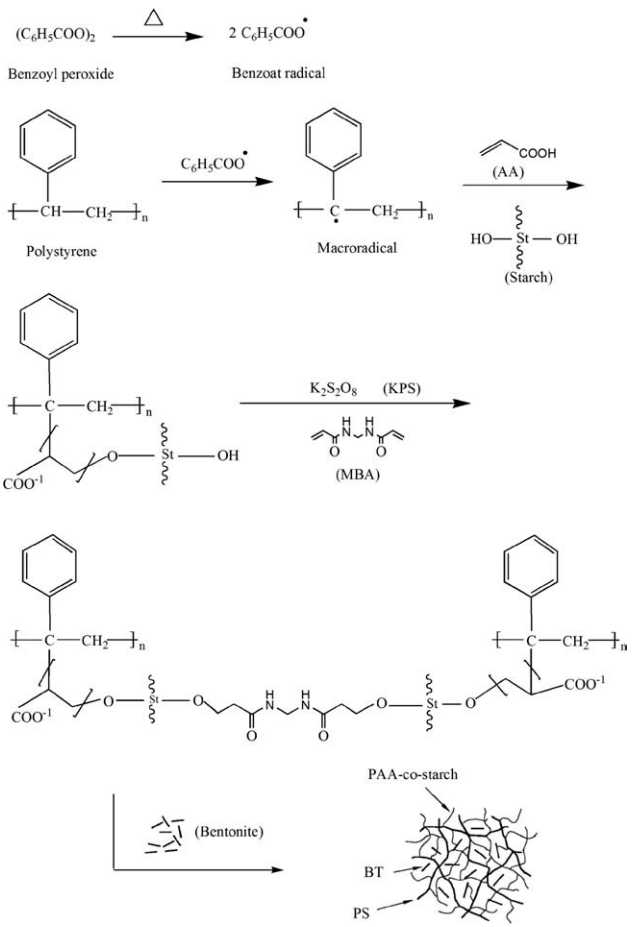


**Figure 2.** A proposed mechanism for the synthesis of the PS-*g*-PAA-*co*-ST/$BT_1$ superabsorbent hydrogel.

**Table I.** Effect of Different Parameters on the Water Absorbencies of PS-*g*-PAA-*co*-ST Superabsorbent

| Sample | AA/PS | Neutralization degree of AA (%) | Starch (wt %) | MBA (wt %) | BP (wt %) | KPS (wt %) | $Q_{eq}$ |
|---|---|---|---|---|---|---|---|
| 1. Effect of AA to PS weight ratio | | | | | | | |
| A | 5 | 70 | 0.10 | 0.08 | 0.80 | 0.80 | 230 |
| B | 7 | 70 | 0.10 | 0.08 | 0.80 | 0.80 | 300 |
| C | 9 | 70 | 0.10 | 0.08 | 0.80 | 0.80 | 390 |
| D | 11 | 70 | 0.10 | 0.08 | 0.80 | 0.80 | 290 |
| E | 13 | 70 | 0.10 | 0.08 | 0.80 | 0.80 | 250 |
| 2. Effect of neutralization degree of AA | | | | | | | |
| A | 9 | 50 | 0.10 | 0.08 | 0.80 | 0.80 | 290 |
| B | 9 | 60 | 0.10 | 0.08 | 0.80 | 0.80 | 330 |
| C | 9 | 70 | 0.10 | 0.08 | 0.80 | 0.80 | 390 |
| D | 9 | 80 | 0.10 | 0.08 | 0.80 | 0.80 | 230 |
| E | 9 | 90 | 0.10 | 0.08 | 0.80 | 0.80 | 180 |
| 3. Effect of starch content | | | | | | | |
| A | 9 | 70 | 0.05 | 0.08 | 0.80 | 0.80 | 370 |
| B | 9 | 70 | 0.10 | 0.08 | 0.80 | 0.80 | 390 |
| C | 9 | 70 | 0.15 | 0.08 | 0.80 | 0.80 | 230 |
| D | 9 | 70 | 0.20 | 0.08 | 0.80 | 0.80 | 190 |
| E | 9 | 70 | 0.25 | 0.08 | 0.80 | 0.80 | 150 |
| 4. Effect of oil-soluble initiator (BP) | | | | | | | |
| A | 9 | 70 | 0.10 | 0.08 | 0.20 | 0.80 | 140 |
| B | 9 | 70 | 0.10 | 0.08 | 0.40 | 0.80 | 165 |
| C | 9 | 70 | 0.10 | 0.08 | 0.60 | 0.80 | 250 |
| D | 9 | 70 | 0.10 | 0.08 | 0.80 | 0.80 | 390 |
| E | 9 | 70 | 0.10 | 0.08 | 1.00 | 0.80 | 350 |
| 5. Effect of water soluble initiator (KPS) | | | | | | | |
| A | 9 | 70 | 0.10 | 0.08 | 0.80 | 0.00 | 180 |
| B | 9 | 70 | 0.10 | 0.08 | 0.80 | 0.40 | 230 |
| C | 9 | 70 | 0.10 | 0.08 | 0.80 | 0.60 | 260 |
| D | 9 | 70 | 0.10 | 0.08 | 0.80 | 0.80 | 390 |
| E | 9 | 70 | 0.10 | 0.08 | 0.80 | 1.00 | 350 |
| 6. Effect of crosslinker content | | | | | | | |
| A | 9 | 70 | 0.10 | 0.04 | 0.80 | 0.80 | 355 |
| B | 9 | 70 | 0.10 | 0.06 | 0.80 | 0.80 | 370 |
| C | 9 | 70 | 0.10 | 0.08 | 0.80 | 0.80 | 390 |
| D | 9 | 70 | 0.10 | 0.10 | 0.80 | 0.80 | 280 |
| E | 9 | 70 | 0.10 | 0.12 | 0.80 | 0.80 | 190 |

$Q_{eq}$: equilibrium water absorbency, (g/g).

during the polymerization process.[36] Because MBA as a crosslinker is present in the reaction, a crosslinked structure is formed. MBA is a bifunctional crosslinker, and after the initiator is added to the solution, a crosslinker macroradical is formed which contains four reactive sites. These active sites can link with the radicals on the acrylic acid, starch, and polystyrene. It should be mentioned that in Figure 2 only two active sites on MBA are shown. Pourjavadi et al. recently reported a similar mechanism for k-carrageenan grafted acrylic acid-*co*-2-acrylamido-2-methylpropanesulfonic acid.[37] The bentonite particles were dispersed among the polymeric network, and the bentonite particles acted as a crosslinking agent. In addition, the FTIR results show that there are interactions between the OH groups of bentonite and the functional groups (C—O and —$COO^-$) of PS-*g*-PAA-*co*-ST.

### Influence of the Weight Ratio of Acrylic Acid to Polystyrene on Water Absorbency

Table I shows that the water absorbency increased with increasing AA content. The maximum swelling capacity was obtained

when the sample was synthesized with an AA to PS mass ratio of 9: 1. This could be due to the fact that the increase in the amount of AA from the ratio of 5: 1 to 9: 1 resulted in an increase in the molecular weight and grafting of poly acrylic acid chains.[26] With further increases in the AA content, the water absorbency decreased. This could be due to (a) preferential homopolymerization of acrylic acid over graft copolymerization or (b) increased medium viscosity which hinders the movement of monomer molecules and free radicals.[38]

### Influence of the Neutralization Degree of AA on Water Absorbency

The effect of the neutralization degree of AA on water absorbency is shown in Table I. The water absorbency increases as the neutralization degree increases from 50 to 70%, and decreases with further increases in the neutralization degree of AA. The maximum water absorbency is obtained when the neutralization degree of the AA is 70%. When acrylic acid was neutralized with a sodium hydroxide solution, the negatively charged carboxyl groups attached to the polymer chains produced an electrostatic repulsion, resulting in an expansion of the network. The electrostatic repulsion rose as the neutralization degree increased from 50 to 70%, leading to increased water absorbency. The further increase in the neutralization degree of AA resulted in the decreased water absorbency of the prepared superabsorbent. This behavior could be due to a rise in chain stiffness and counter ion condensation on the polyion.[39] We believe that due to the increased amount of counter ion ($Na^+$) with increasing AA neutralization degree, the condensation of counter ions that cover $COO^-$ ions increased, resulting in a decreased formation of hydrogen bonds between the $COO^-$ groups and $H_2O$. This phenomenon causes the water absorbency of the superabsorbent hydrogel to decrease.

### Influence of Starch Content on Water Absorbency

Table I shows the effect of different amounts of starch on water absorbency in distilled water. It can be seen that the amount of starch powder used has an important role in the equilibrium water absorbency of the prepared samples. The water absorbency increased from 370 to 390 g/g as the ratio of starch in the feed increased from 0.05 to 0.1 wt %, and further increases in the amount of starch in the feed decreased the water absorbency. According to a previous study,[8] wheat straw can react with AA to enhance the polymeric network. A similar mechanism may have played a role in this study; starch contains a number of hydrophilic functional groups (—OH groups), and thus reactions between the OH groups of starch and the $COO^{-1}$ groups of AA may occur and enhance the polymeric network resulting in an increase in water absorbency.[8] When the starch content was >0.1% in the feed, the water absorbency decreased. This phenomenon could be due to the generation of more crosslink points in the polymeric network which would cause the crosslink density of the superabsorbent hydrogel to increase; therefore, there should be a decrease in the water absorbency.[8]

### Influence of Initiator Content on Water Absorbency

Table I illustrates the effect of the oil-soluble initiator and water-soluble initiator on the water absorbency of the prepared samples. The water absorbency increases as the BP and KPS contents increase from 0.2 to 0.8% and from 0.0 to 0.8%, respectively, but decreases with further increases in the BP and KPS content. The maximum water absorbency (390 g/g) is obtained when the total amount of initiator (KPS and BP) is 1.6% which causes the graft polymerization rate to increase; consequently, the final water absorbency increases. When the total amount of initiator is higher than the optimum value, the water absorbency decreases. This phenomenon is most likely due to an increase in the number of radical centers, which increases the crosslinking density. The greater crosslinking density prevents the network from expanding to its greatest extent. Furthermore, an increase in the number of radical centers leads to a decrease in the chain length of the grafted AA-*co*-starch of the hydrogel and a decrease in the molecular weight of the grafted AA-*co*-starch of the hydrogel. As a result, the water absorbency decreases. This may be attributed to the inverse relationship between the initiator content and molecular weight.[37]

**Table II.** Effect of Sodium Bentonite Content on the Water Absorbencies of the Superabsorbent Composites[a]

| Sample | Bentonite percentage (wt %) | $Q_{H2O}$ (g/g) | |
|---|---|---|---|
| | | Distilled water | NaCl (0.9 wt %) |
| PS-*g*-PAA-*co*-ST/$BT_0$ | 0 | 390 | 42 |
| PS-*g*-PAA-*co*-ST/$BT_1$ | 3 | 500 | 49 |
| PS-*g*-PAA-*co*-ST/$BT_2$ | 5 | 350 | 45 |
| PS-*g*-PAA-*co*-ST/$BT_3$ | 7 | 315 | 40 |
| PS-*g*-PAA-*co*-ST/$BT_4$ | 9 | 280 | 38 |
| PS-*g*-PAA-*co*-ST/$BT_5$ | 11 | 260 | 33 |

[a]Reaction conditions: reaction temperature, 70°C; 70% neutralization degree of AA; weight ratio of AA/PS in the feed 9 : 1; weight ratios of starch, oil-soluble initiator, water-soluble initiator and crosslinker in the feed of 0.10, 0.80, 0.80, and 0.08 wt %, respectively.

### Influence of Crosslinker Content on Water Absorbency

Table I shows the effect of the crosslinker content on water absorbency. An increase in the crosslinker content from 0.08 to 0.12% leads to a decreased water absorbency. This phenomenon is most likely due to the fact that, as the amount of crosslinker increases, more crosslink points are produced during polymerization and the crosslinking density increases. The increased crosslinking density leads to a highly crosslinked and rigid structure, and the polymer network can not expand enough to retain a large amount of water. The maximum water absorbency is achieved when the amount of crosslinker is 0.08%. When the amount of crosslinker is <0.08%, the water absorbency decreases due to an increase in soluble materials.[26] This tendency is similar to that of the starch-graft-poly acrylic acid/attapulgite superabsorbent prepared by Li et al.[26]

### Influence of Bentonite Content

The influence of bentonite content on the water absorbency of the PS-*g*-PAA-*co*-ST/BT superabsorbent composite is shown in Table II. It is obvious that the BT content has an important effect on the water absorbency of the superabsorbent composite.

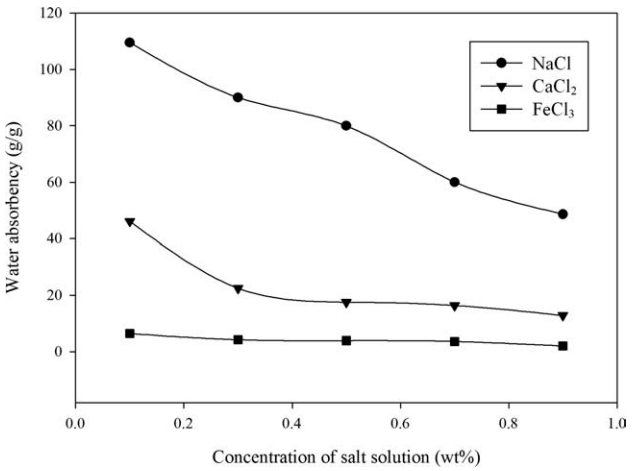


**Figure 3.** Water absorbency of PS-*g*-AA-*co*-ST/$BT_1$ in NaCl, $CaCl_2$, and $FeCl_3$ in aqueous solutions with various salt concentrations.

The water absorbency of the superabsorbent composite in distilled water and in 0.9 wt % NaCl solution increased from 390 to 500 g/g and from 42 to 49 g/g, respectively, as 3 wt % BT was introduced. According to the data from the IR analysis of this work, the —OH groups of BT could participate in the formation of the composite, which can enhance the polymeric network and increase the water absorbency. Furthermore, Na-bentonite (BT) contains $Na^+$ cations that are almost completely dispersed into the composite polymeric network, thus increasing the hydrophilicity of the composite and causing the water absorbency to increase.[9] A further increase in the BT content to 11 wt % leads to a decreased water absorbency of 260 in distilled water and 33 g/g in 0.9 wt% NaCl solution. The water absorbency decreased with increasing BT content. This could be due to the fact that the interactions among the BT, acrylic acid, and starch increase gradually with increasing BT content, which leads to an increased formation of physical and chemical cross-links in the polymeric network. With more physical and chemical cross-links in the polymeric network, the elasticity of the polymer chains decreases. The water absorbency of the superabsorbent composite decreases with decreasing polymer elasticity.[9]

### Effect of Salt Solution on Water Absorbency

The effect of saline solution on water absorbency is shown in Figure 3. The swelling capacity of the superabsorbent in saline solutions was lower than that in distilled water. This phenomenon could be due to a charge screening effect of the excess cations. The excess cations can shield the carboxylate anions and decrease the effective anion–anion repulsion, resulting in a decrease in the osmotic pressure (ionic pressure) difference between the hydrogel network and the external solution.[40] As shown in Figure 3, the swelling capacity of the prepared hydrogel in the prepared saline solutions is $Na^+ > Ca^{2+} > Fe^{+3}$. The absorbency of the superabsorbent composites in the salt solutions is monovalent > divalent > trivalent cations; the degree of ionic crosslinking increases with increasing cation charge, and consequently, swelling decreases.[37] The reduced water-absorbing capacity observed in multivalent cationic solutions can be attributed to the carboxylate groups, which can induce the formation of intermolecular and intramolecular complexes, resulting in an increase in the network crosslinking density.[41] The ability of the carboxylate group to form a complex with the three cations is $Fe^{3+} > Ca^{2+} > Na^+$, based on their formation constants for ethylenediaminetetraacetic acid (EDTA).[17] In addition, the water absorbency decreases with increasing concentrations of different external saline solutions. This phenomenon may be due to the presence of cations in different salt solutions. The osmotic pressure between the external saline solution and the polymeric network decreases with increasing concentration of the saline solution.[42] The penetration of counter ions ($Fe^{+3}$, $Ca^{2+}$, and $Na^{+1}$) in the polymeric network can have a screening effect on the carboxylate groups (—$COO^-$), which results in a decreased water absorbency of the superabsorbent composites.[40]

### Morphological Analysis

The porosity of a hydrogel can affect its water absorbency and retention rate.[40] Thus, one of the important properties to investigate is the hydrogel microstructure morphology. SEM micrographs of PS-*g*-PAA-*co*-ST/$BT_0$ and PS-*g*-PAA-*co*-ST/$BT_1$ are shown in Figure 4. These images confirm that the prepared samples have a porous structure. The surface of the PS-*g*-PAA-*co*-ST/$BT_1$ composite seems to be more porous (higher pore

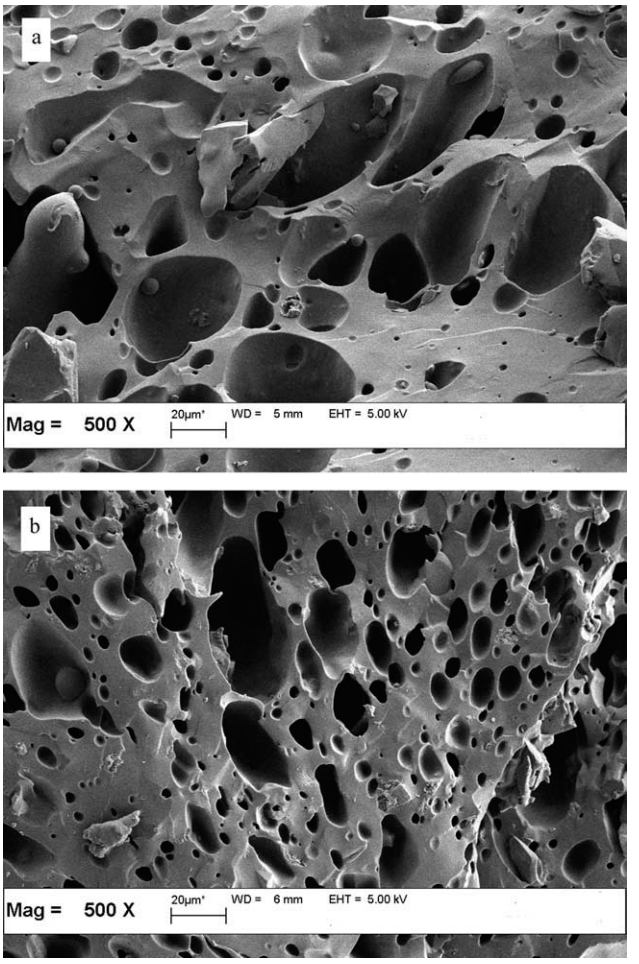


**Figure 4.** Scanning electron micrographs of (a) PS-*g*-PAA-*co*-ST/$BT_0$ and (b) PS-*g*-PAA-*co*-ST/$BT_1$.

density) than that of PS-*g*-PAA-*co*-ST/$BT_0$. It can be concluded from the SEM images that the bentonite particles were well dispersed in the composite; thus, there is a good interaction between the clay particles and the polymer chains. In addition, these pores should provide regions for water penetration into the polymeric network and interaction sites for the hydrophilic groups of the polymer network and external stimuli.[9,37]

### Thermal Stability

Figure 5 shows the thermal decomposition of PS-*g*-PAA-*co*-ST/$BT_0$ and PS-*g*-PAA-*co*-ST/$BT_1$. Both superabsorbents passed through three steps from room temperature to 700°C, but there were some differences between the two samples in each step. The temperatures for 10% weight loss for PS-*g*-PAA-*co*-ST/$BT_1$ and PS-*g*-PAA-*co*-ST/$BT_0$ were 261 and 242°C, respectively. Although the maximum decomposition for both samples occurred at the third step, the maximum decomposition temperature ($T_{max}$) in the third step for PS-*g*-PAA-*co*-ST/$BT_1$ was higher (467°C with 52% weight loss) than that of PS-*g*-PAA-*co*-ST/$BT_0$, which was 453°C with 58% weight loss. The experimental data show that the total percentage weight loss of the PS-*g*-PAA-*co*-ST/$BT_1$ superabsorbent was lower than that of PS-*g*-PAA-*co*-ST/$BT_0$. Furthermore, the initial decomposition temperature and the maximum decomposition temperature of each step for PS-*g*-PAA-*co*-ST/$BT_1$ were higher than those of PS-*g*-PAA-*co*-ST/$BT_0$. This indicates that the incorporation of bentonite into the polymer network leads to an increase in thermal stability. This phenomenon occurs due to the heat barrier effect of bentonite which enhanced the thermal stability of the sample.

### Swelling Rate

The swelling rates of the PS-*g*-PAA-*co*-ST/$BT_0$ and PS-*g*-PAA-*co*-ST/$BT_1$ superabsorbents were determined and are illustrated in Figure 6. It can be seen from Figure 6 that the swelling rates of PS-*g*-PAA-*co*-ST/$BT_0$ and PS-*g*-PAA-*co*-ST/$BT_1$ were higher for 0–35 min and that the water absorbency of PS-*g*-PAA-*co*-ST/$BT_0$ and PS-*g*-PAA-*co*-ST/$BT_1$ reached 280 and 360 g/g within 35 min, respectively. Then the swelling rates decreased slowly, and the equilibrium water absorbency of PS-*g*-PAA-*co*-ST/$BT_0$ and PS-*g*-PAA-*co*-ST/$BT_1$ was reached within 90 and 125 min, respectively. Compared with the swelling of PS-*g*-PAA-*co*-ST/$BT_0$, the swelling of the PS-*g*-PAA-*co*-ST/$BT_1$ superabsorbent took longer to reach equilibrium. The swelling rate of a superabsorbent is determined by the surface area, swelling ability, polymer density, and particle size.[43] The higher swelling equilibrium rate for PS-*g*-PAA-*co*-ST/$BT_0$ could be due to the fact that the superabsorbent without clay has a looser polymeric network in comparison to the superabsorbent with clay, PS-*g*-PAA-*co*-ST/$BT_1$. Furthermore, the introduced bentonite particles blocked the penetration of distilled water into the superabsorbent composite, so the time required to achieve the swelling equilibrium for PS-*g*-PAA-*co*-ST/$BT_1$ was greater than that for PS-*g*-PAA-*co*-ST/$BT_0$. A similar observation was reported by Wang et al. for the preparation of poly acrylic acid-*co*-acryl amide/sodium humate/attapulgite.[17]

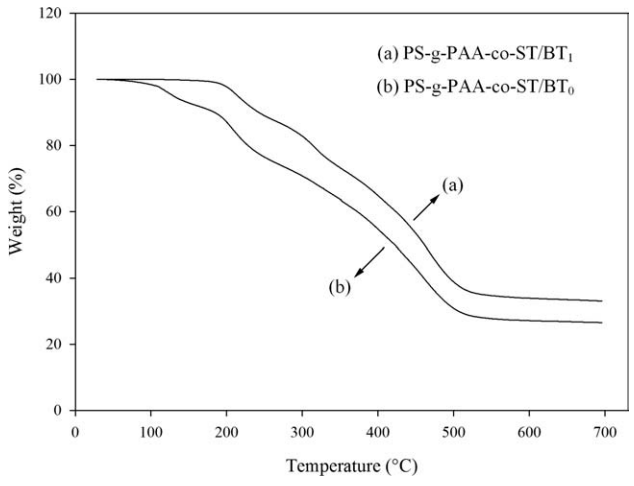


**Figure 5.** TGA curves of (a) PS-*g*-PAA-*co*-ST/$BT_1$ and (b) PS-*g*-PAA-*co*-ST/$BT_0$ at a heating rate of 10°C $min^{-1}$.

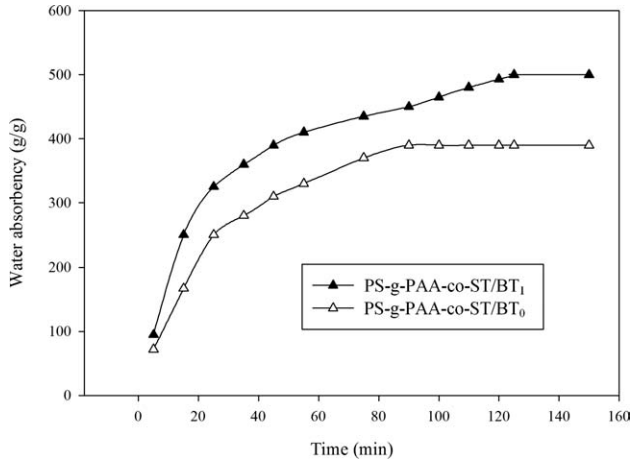


**Figure 6.** Swelling rate in distilled water for PS-*g*-PAA-*co*-ST/$BT_0$ and PS-*g*-PAA-*co*-ST/$BT_1$.

## CONCLUSIONS

A superabsorbent hydrogel was prepared by the graft copolymerization of AA and starch onto polystyrene through emulsion polymerization. The maximum water absorbency under optimum conditions for PS-*g*-PAA-*co*-ST/$BT_1$ was 500 g/g in distilled water and 49 g/g in NaCl solution (0.9 wt % NaCl). The results from FTIR indicated that the —OH groups of starch and BT and the —$COO^-$ groups of AA participated in graft polymerization on polystyrene backbone chains. The SEM results showed that the small bentonite particles can disperse in the polymer network. TGA investigations demonstrated that the introduction of bentonite particles can improve the thermal stability of the prepared sample. Furthermore, the use of waste polystyrene not only can reduce the production cost of superabsorbent hydrogel, but can also provide a new method for converting waste resources into valuable products.

## ACKNOWLEDGMENTS

The authors wish to acknowledge the financial support provided by a USM short-term grant (Ac No.: 8044043). Maryam Irani thanks Universiti Sains Malaysia for its financial support under the USM fellowship scheme for her PhD study.

## REFERENCES


1. Yang, H.-S.; Yoon, J.-S.; Kim, M.-N. *Polym. Degrad. Stab.* **2005,** *87*, 131.
2. Gao, Y.; Li, H.; Wang, X. *Eur. Polym. J.* **2007,** *43*, 1258.
3. Subramanian, S.; Lee, S. *J. Appl. Polym. Sci.* **1998,** *70*, 1001.
4. Subramanian, S.; Lee, S. *Polym. Eng. Sci.* **1999,** *39*, 2274.
5. Bergbreiter, D. E.; Zhong, Z. *Ind. Eng. Chem. Res.* **2005,** *44*, 8616.
6. Bajdur, W.; Pajaczkowska, J.; Makarucha, B.; Sulkowska, A.; Sulkowski, W. W. *Eur. Polym. J.* **2002,** *38*, 299.
7. Teli, M. D.; Waghmare, N. G. *Carbohydr. Polym.* **2010,** *81*, 695.
8. Liang, R.; Yuan, H.; Xi, G.; Zhou, Q. *Carbohydr. Polym.* **2009,** *77*, 181.
9. Zhang, J.; Wang, L.; Wang, A. *Ind. Eng. Chem. Res.* **2007,** *46*, 2497.
10. Singh, B.; Sharma, N. *Polym. Degrad. Stab.* **2007,** *92*, 876.
11. Mostafa, K. M. *Polym. Degrad. Stab.* **1997,** *55*, 125.
12. El-Rafie, M. H.; Zahran, M. K.; El Tahlawy, K. F.; Hebeish, A. *Polym. Degrad. Stab.* **1995,** *47*, 73.
13. Athawale, V. D.; Lele, V. *Carbohydr. Polym.* **1998,** *35*, 21.
14. Lu, S.; Duan, M.; Lin, S. *J. Appl. Polym. Sci.* **2003,** *88*, 1536.
15. Sugahara, Y.; Ohta, T. *J. Appl. Polym. Sci.* **2001,** *82*, 1437.
16. Athawale, V. D.; Lele, V. *Carbohydr. Polym.* **2000,** *41*, 407.
17. Zhang, J. P.; Li, A.; Wang, A. Q. *Polym. Adv. Technol.* **2005,** *16*, 813.
18. Raju, K. M.; Raju, M. P. *Adv. Polym. Tech.* **2001,** *20*, 146.
19. Zhou, W.-J.; Yao, K.-J.; Kurth, M. J. *J. Appl. Polym. Sci.* **1996,** *62*, 911.
20. Yao, K. J.; Zhou, W. J. *J. Appl. Polym. Sci.* **1994,** *53*, 1533.
21. Yin, L.; Zhao, X.; Cui, L.; Ding, J.; He, M.; Tang, C.; Yin, C. *Food. Chem. Toxicol.* **2009,** *47*, 1139.
22. Yin, L.; Zhao, Z.; Hu, Y.; Ding, J.; Cui, F.; Tang, C.; Yin, C. *J. Appl. Polym. Sci.* **2008,** *108*, 1238.
23. Dzinomwa, G. P. T.; Wood, C. J.; Hill, D. J. T. *Polym. Adv. Technol.* **1997,** *8*, 767.
24. Lokhande, H. T.; Gotmare, V. D. *Bioresour. Technol.* **1999,** *68*, 283.
25. Kabiri, K.; Zohuriaan-Mehr, M. J. *Polym. Adv. Technol.* **2003,** *14*, 438.
26. Li, A.; Zhang, J.; Wang, A. *Bioresour. Technol.* **2007,** *98*, 327.
27. Lee, W.-F.; Chen, Y.-C. *Eur. Polym. J.* **2005,** *41*, 1605.
28. Liu, P.-S.; Li, L.; Zhou, N.-L.; Zhang, J.; Wei, S.-H.; Shen, J. *J. Appl. Polym. Sci.* **2007,** *104*, 2341.
29. De Graaf, R. A.; Janssen, L. P. B. M. *Polym. Eng. Sci.* **2000,** *40*, 2086.
30. Anirudhan, T. S.; Suchithra, P. S.; Rijith, S. *Colloids Surf. A* **2008,** *326*, 147.
31. Teli, M. D.; Waghmare, N. G. *Carbohydr. Polym.* **2009,** *78*, 492.
32. Pal, S.; Mal, D.; Singh, R. P. *Carbohydr. Polym.* **2005,** *59*, 417.
33. Zhirong, L.; Azhar Uddin, M.; Zhanxue, S. *Spechtrochim. Acta A* **2011,** *79*, 1013.
34. Chen, G.; Liu, S.; Chen, S.; Qi, Z. *Macromol. Chem. Phys.* **2001,** *7*, 1189.
35. Faravelli, T.; Pinciroli, M.; Pisano, F.; Bozzano, G.; Dente, M.; Ranzi, E. *J. Anal. Appl. Pyrol.* **2001,** *60*, 103.
36. Peter Robinson, N. V.-D. US Patent 4,739,008, **1988.**
37. Pourjavadi, A.; Barzegar, S.; Zeidabadi, F. *React. Funct. Polym.* **2007,** *67*, 644.
38. Pourjavadi, A.; Harzandi, A. M.; Hosseinzadeh, H. *Eur. Polym. J.* **2004,** *40*, 1363.
39. Ende, M. T.; Hariharan, D.; Peppas, N. A. *React. Polym.* **1995,** *25*, 127.
40. Bao, Y.; Ma, J.; Li, N. *Carbohydr. Polym.* **2011,** *84*, 76.
41. Castel, D.; Ricard, A.; Audebert, R. *J. Appl. Polym. Sci.* **1990,** *39*, 11.
42. Murali Mohan, Y.; Keshava Murthy, P. S.; Mohana Raju, K. *React. Funct. Polym.* **2005,** *63*, 11.
43. Elliott, J. E.; Macdonald, M.; Nie, J.; Bowman, C. N. *Polymer* **2004,** *45*, 1503.